Applied Physics Letters

Resonant metasurface with tunable asymmetric reflection

Cite as: Appl. Phys. Lett. **113**, 094103 (2018); https://doi.org/10.1063/1.5046948
Submitted: 03 July 2018 . Accepted: 14 August 2018 . Published Online: 29 August 2018

Dmitry Filonov, Vitali Kozlov, Andrey Shmidt, Ben Z. Steinberg, and Pavel Ginzburg

Resonant metasurface with tunable asymmetric reflection

Dmitry Filonov,[1,2,3,a)] Vitali Kozlov,[1,2] Andrey Shmidt,[1] Ben Z. Steinberg,[1] and Pavel Ginzburg[1,2]
[1]School of Electrical Engineering, Tel Aviv University, Tel Aviv 69978, Israel
[2]Light-Matter Interaction Centre, Tel Aviv University, Tel Aviv 69978, Israel
[3]ITMO University, St. Petersburg 197101, Russia

(Received 3 July 2018; accepted 14 August 2018; published online 29 August 2018)

Suppression of backscattered electromagnetic waves by carefully designed structures is highly demanded in a range of applications, some of which are radar invisibility, antenna isolation, and many others. Salisbury screens, composed of a mirror with an additional layer on top, are traditionally used for these purposes. Here, we report on the design and experimental demonstration of a reciprocal screen, which demonstrates asymmetric reflection properties when illuminated from opposite directions. The structure utilizes near-field magneto-electric coupling between subwavelength split ring resonators and wires, forming a metasurface. While the reciprocal structure demonstrates perfect symmetry in transmission, strong backscattered asymmetry is shown to be controllable by carefully choosing the Ohmic losses, which are implemented with lumped resistors soldered into the resonators. Depending on the load, the meta-screen demonstrates switching properties that vary between fully symmetric and completely asymmetric reflection between the forward and backward directions of incident illumination. The frequency selective surface acts as a Huygens element when illuminated from one side and as a perfect mirror when illuminated from the other. The ability to tailor the asymmetric reflectance of electromagnetic metasurfaces by controlling Ohmic losses allows employing additional degrees of freedom in designing of radomes and other antenna devices. Furthermore, the concept could be extended to optical frequencies, where resistive losses can be controlled via direct carrier injection into semiconductor devices. *Published by AIP Publishing.*
https://doi.org/10.1063/1.5046948

Suppression of electromagnetic scattering from structures, especially in the backward direction, has been attracting continuous attention since before the 1960s, when radar invisibility technologies started to emerge.[1] One celebrated example of backscattering suppression includes the Salisbury screen, composed of a ground plane and a thin absorption layer, located at a distance of a quarter wavelength above it. As a result of the incident field's interaction with the structure, the reflected wave is efficiently absorbed in the layer and therefore backscattering is supressed. Concepts of this type of antireflection coating can be further extended to many different geometries, aiming to maximize the operational bandwidth and widen the functionality for a broader range of incident angles, have been thoroughly considered in the literature.[2–5] Other notable examples of anti-reflection screens are the Dullenbach shield[6,7] and the Jaumann absorber.[8] In general, Frequency Selective Surfaces (FSSs) with properly designed periodicities, capable of suppressing secondary diffraction orders, are extensively used in many applications.[9] Furthermore, the bianisotropy properties of structured surfaces were shown to supress spurious diffraction orders.[10] During the last decades, the concept of metasurfaces, which at this context can be viewed as overpopulated FSSs, started to develop. While the initial starting point of this research direction was a demonstration of on demand capabilities to manipulate visible light (e.g., Refs. 11–14), the concept was found to be very powerful for centimetre and millimetre wave designs (e.g., Refs. 15–19 also in application to thin perfectly absorbing layers[20,21]). One of the main contributions of the metasurface approach is to provide the ability of controlling the local phase of electromagnetic radiation and, as a result, tailor its reflection and refraction properties. An example of a metasurface based Salisbury screen was reported in Ref. 22. Special attention was paid to nonreciprocal metasurfaces, which allowed achieving a high level of isolation by, for example, allowing transmission through the layer from one side, while blocking the wave coming from the opposite direction.[23] In contrast, the structure reported here obeys the reciprocity principle, as will be underlined hereafter.

The operation principle of the proposed structure is schematically illustrated in Fig. 1. The electromagnetic wave interacts with the metasurface bi-layer, composed of an array of split ring resonators (SRRs) and electric wires. The reflection from the array depends on the incident direction—being illuminated from one side, the structure acts as a so-called Huygens surface,[24,25] which suppresses back reflection. However, if the direction of incidence is flipped, the device acts as a mirror, reflecting the entire incident wave. It will be shown that this type of asymmetry depends on resistive losses and can be controlled by varying their nominals. As a result, the whole effect can possess tuneable behaviour. Those two aspects set the distinguishable differences and advantages of the proposed device over traditional inherently non-transparent Salisbury screens and allow additional valuable functionalities in controlling the electromagnetic interactions.

a)dimfilonov@gmail.com

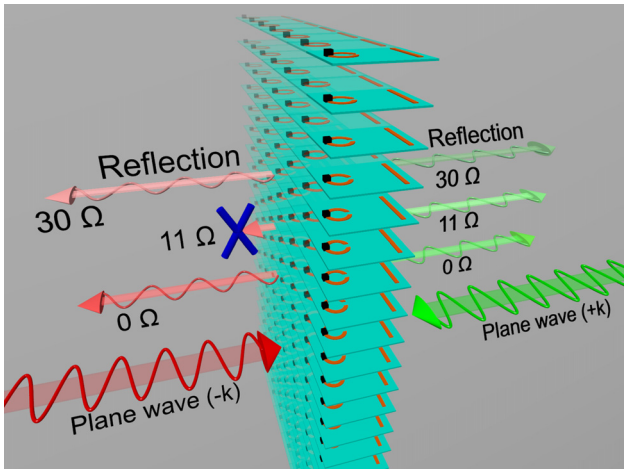

FIG. 1. Schematic representation of the basic operation principles of the metasurface with tuneable asymmetric reflection. Electromagnetic waves, incident either from the left or from the right are depicted with red and green colours, respectively. Different reflection scenarios are marked with nominal values of resistive elements lumped into split ring resonators (SRRs). For a certain range of resistances, the reflection is strongly asymmetric.

The manuscript is organized as follows: general discussion and numerical design of the metasurface will be demonstrated at first followed by the experimental verification. Discussion and outlook will conclude the report.

Magneto-electric interaction is an effective coupling mechanism between a pair of closely situated magnetic and electric dipoles. Metal split ring resonators and half-wavelength wires were taken for the practical realization of those basic elements. The coupling mechanism was investigated in, e.g., Refs. 26 and 27, where it was shown that the scattered electric field of the SRR couples to the wire, while the wire couples back to the SRR with its magnetic field. This analysis includes time retardation effects, hence electric and magnetic fields are mutually coupled. The magneto-electric coupling, in contrast, e.g., to the case of coupled electric dipoles, is fundamentally dependent on the propagation direction of the excitation, since the magnetic field must flip its sign under the time-reversal transformation. Based on this concept, the hybrid magneto-electric particle with asymmetric backscattering properties has been demonstrated. It is worth noting, that the strong asymmetry factor in the case of an isolated structure, is attributed to the far-field scattering diagram and not to the reflection coefficients, which are not well-defined in the case of a standalone magneto-electric particle. Furthermore, the detailed analysis shows that far-field radiation damping is required for achieving the effect. Here, the infinite array of hybrid magneto-electric particles is considered and optimized towards the asymmetric reflection performance. The mutual coupling between neighbouring elements was taken into account and both the geometry of the unit cell and the period were optimised towards achieving the maximal asymmetry factor. The starting point for the optimization was the array of magneto-electric particles, taken as if they are not mutually interacting.[26,27] It is worth noting, that infinitely overpopulated arrays of resonators do not have diffraction orders and, as a result, Ohmic losses should be introduced as a dissipation channel. This loss-assisted asymmetry phenomenon will be analysed hereafter.

The performance of the optimised structure appears in Fig. 2, where absolute values for transmission and reflection coefficients are demonstrated as the function of frequency. Resistive loads were implemented as lumped elements, plugged within the second gap of the SRR (Fig. 1). Four different values have been considered—0, 1, 5, and 13 Ω. The geometry of the unit cell appears in Fig. [4(b), inset]. The substrate is taken to be similar to lossless FR4 ($\epsilon_r = 4.3$ and 1.5 mm thick), while the 0.1 mm thick metallic strips were assumed to be made of a perfect electric conductor. This idealized structure was considered first for demonstration of the basic effect. The structure was analysed numerically with CST Microwave Studio. Periodic boundary conditions were applied along with a pair of waveguide ports in order to calculate transmission and reflection coefficients of the infinite array.

The reciprocal behaviour of the device can be seen in Fig. 2(a), where exactly the same transmission is obtained for opposite incident directions. Since the device is made from passive, linear, and not magnetically biased components, this behaviour is expected. On the other hand, the case of reflection is completely different, as the reciprocity principle does not apply to the backscattered signal. Here, Figs. 2(b) and 2(c) should be compared. Since the overall energy of the wave is conserved and the transmission does not depend on the incidence direction, asymmetric losses immediately imply the asymmetric reflection. The comparison between the reflection coefficients,

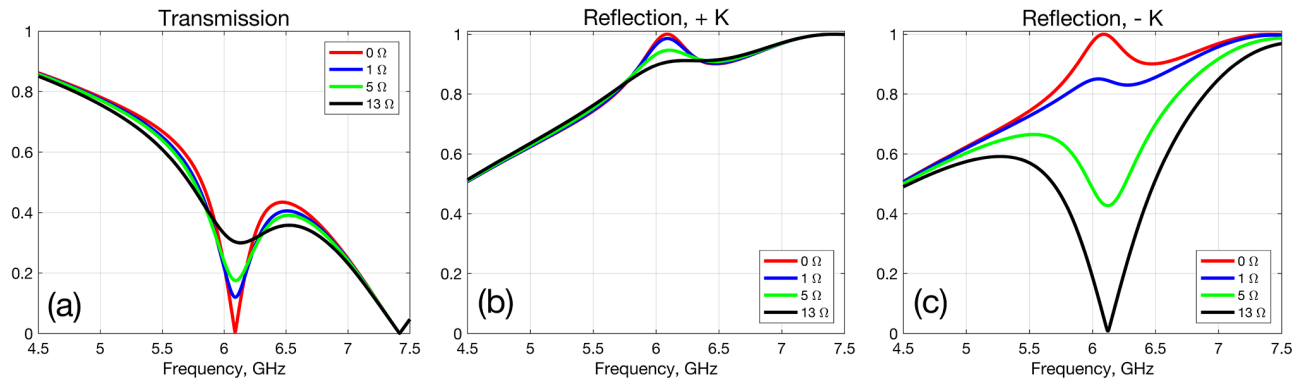

FIG. 2. Transmission-reflection coefficients (for amplitudes) of an infinite magneto-electric metasurface with resistive loads. (a) Transmission spectrum (symmetric for opposite illumination directions owing to the reciprocity). (b) and (c) Reflection spectra for opposite illumination directions, indicated with +k (wire is closer to the source) and −k (split ring resonator is closer) (see Fig. 1). Colour lines correspond to different nominal values of lumped resistors, as indicated in the captions. All other components were assumed to be lossless.

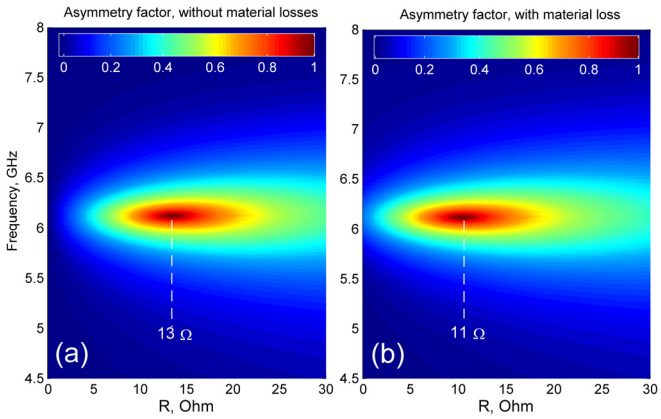

FIG. 3. Colour map of the asymmetry factor, quantifying the difference between reflection coefficients, if the structure is flipped with respect to the direction of the incident illumination. Horizontal axis—the resistive load nominal, vertical axis—the operation frequency. (a) Lossless constitutive elements. (b) Structure with losses in the substrate and metal elements.

shown in Figs. 2(b) and 2(c), demonstrates this behaviour. It is worth noting that without the resistive loads (red lines), the reflection spectra are almost identical. However, introduction of the resistance dramatically changes the balance between the reflection coefficients. Comparison between black lines, corresponding to 13 Ω load, demonstrates the effect. Under "−k" illumination, the structure operates as a resonant Huygens surface (the reflection vanishes), but once illuminated from the opposite side, it behaves as a reflector with 90% efficiency. As in the case of the Huygens element, magnetic and electric dipoles within the structure are resonantly excited and destructively interfere in the backward direction.

In order to study the influence of the resistive load on the asymmetric reflection, an asymmetry factor, similar to the visibility function in optics, is introduced as $V = \frac{R_{+k}-R_{-k}}{R_{+k}+R_{-k}}$. This normalized ratio is bounded between 0 and 1, since it is defined with the help of the absolute values of reflection amplitude coefficients $[R, T \in (0, 1)]$. Note that $R_{+k} \geq R_{-k}$. Figure 3 shows the colour map of the reflection asymmetry factor (numerical value), as a function of the incident frequency and resistive load. The data from Fig. 2 corresponds to four vertical cuts of this colour map. The asymmetry factor has a clear maximum around 6.25 GHz (where the resonant response was designed) and a 13 Ω load. The data clearly shows that the asymmetry vanishes without the lumped resistance.

However, if the losses increase, the resonance of the whole structure experiences a slight shift towards higher frequencies. The more important effect is that the quality factor/interaction between the magnetic and electric dipoles within the unit cell drops down. As a result, the asymmetry disappears, and the reflection coefficients tend to become symmetric again. This behaviour is somehow similar to the operation of a perfectly conducting mirror—despite having infinite conductivity, the structure has no losses, since the electromagnetic field does not penetrate inside the lossy material. Note that in our structure case, the transmission does not go to zero, in contrast to the perfect mirror case.

Losses within the substrate and metallic elements also play a role. In order to verify their importance, we introduced them into the previous lossless model. The loss tangent of the substrate is taken to be 0.025 and copper conductivity is 5.96 $\times$ 10^3 S/m. The asymmetry factor for this structure appears in Fig. 3(b). Comparison between panels (a) and (b) demonstrates that the losses in the constitutive elements effectively correspond to the additional nominal resistance of 2 Ω, while the asymmetric behaviour of the structure is preserved.

Experimental verification was performed in an anechoic chamber with three similar magneto-electric metasurfaces, which differed only by the nominal value of the resistors that were soldered into gaps of the split ring resonators. The dimensions of the unit cell appear in Fig. 4 (insets). The finite array is based on 10 $\times$ 10 unit cells, etched on a FR4 substrate. The array's response was measured over a band of 5–7.5 GHz using a network analyser, which fed a simultaneously transmitting and receiving horn, located at a distance of 3 m away from the sample array (standard S-parameters measurement). It should be noted that reflection coefficients for a finite size structure, situated in a free space, are not well defined. In contrast, backscattering cross sections were extracted by comparing the reflection with the calibration 38 mm diameter steel sphere. While this technique is used for obtaining real (not normalized) values of scattering cross-sections, lens antenna for quasi-Gaussian beam illumination or waveguide geometries are used to experimentally approach performances of infinite structures. Nevertheless, radar-type of applications fall in the first characterization category (scattering cross section investigation), which was employed here.

Figures 4(a) and 4(b) show the numerically extracted cross sections. It should also be noted that in the case of finite structures, loaded with lumped elements, both Ohmic resistances and radiation losses (e.g., as in the case of a single magneto-electric particle) contribute to the asymmetric

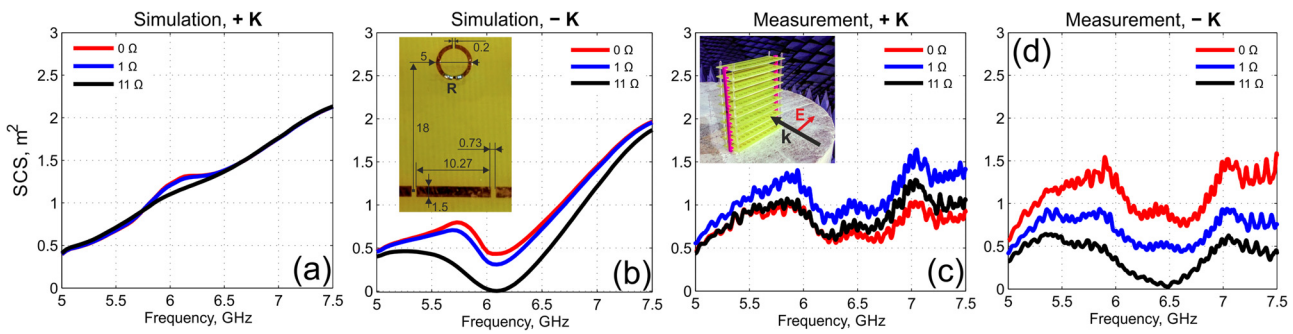

FIG. 4. Backscattering spectra of a 10 $\times$ 10 metasurface magneto-electric particles array. (a) and (b) Full wave simulation of the finite structure. [(b), inset]—Photograph of a unit cell of the structure. (c) and (d) Experimental data. [(c), inset]—Photograph of a fabricated sample, positioned on a foam holder inside the anechoic chamber. Nominal of lumped resistors appears in captions and corresponds to colour lines.

reflection behaviour. This fact explains the asymmetry that exists even when the resistive load vanishes [red curves in Figs. 4(a) and 4(b)]. Comparison between Figs. 2(b) and 2(c) and Figs. 4(a) and 4(b) underlines very close similarities between an ideal infinite array and its finite counterpart, especially at a high resistive load of 11 Ω, where the radiation loss that exists in the finite screen (and absent in the infinite periodic one) becomes less important.

Figures 4(c) and 4(d) show the experimental data. A quite close correspondence between the measurements and full-wave simulation-based predictions (especially in the case of "−k") can be observed. Oscillations on the experimental curves are quite typical and correspond to the multiple reflections from the excitation horn antennas, which are situated in the vicinity of the sample, as well as between diffracted waves at the sample edges.

The concept of asymmetric reflection in magneto-electric metasurfaces was developed and shown to be reliably controllable through resistive losses. The continuous tuning of the reflection asymmetry factor was introduced. It was demonstrated that the structure can possess properties of the Huygens metasurface, being illuminated from one side, while acting as a good mirror if the illumination comes from the opposite direction. The controllable asymmetric reflection can find use in a span of smart electromagnetic devices, such as radar antireflection coatings, antenna array isolators, and more. Moreover, the resistive loss, essential for the asymmetric behaviour, can be controlled electronically with an additional driving circuit, which makes the demonstrated concept fully integrable with larger scale systems. The developed concepts can also be applied to optical devices via the scaling approaches (e.g., Refs. 28–32).

The research was supported in part by the Binational Science Foundation (Project No. 2016059), Kamin Project, and the PAZY Foundation. Experimental studies were partially supported by the Ministry of Education and Science of the Russian Federation (Zadanie Na. 3.2465.2017/4.6).

[1]W. Bahret and C. J. Sletten, "A look into the future of radar scattering," Proc. IEEE **53**(8), 786–795 (1965).
[2]S. A. Tretyakov and S. I. Maslovski, "Thin absorbing structure for all incidence angles based on the use of a high-impedance surface," Microwave Opt. Technol. Lett. **38**(3), 175–178 (2003).
[3]F. C. Seman, R. Cahill, and V. F. Fusco, "Low profile Salisbury screen radar absorber with high impedance ground plane," Electron. Lett. **45**(1), 10–12 (2009).
[4]W. Li, M. Chen, Z. Zeng, H. Jin, and Y. Pei, "Broadband composite radar absorbing structures with resistive frequency selective surface: Optimal design, manufacturing and characterization," Compos. Sci. Technol. **145**, 10–14 (2017).
[5]B. M. Wells, C. M. Roberts, and V. A. Podolskiy, "Metamaterials-based Salisbury screens with reduced angular sensitivity," Appl. Phys. Lett. **105**(16), 161105 (2014).
[6]E. F. Knott, J. F. Shaeffer, and M. T. Tuley, *Radar Cross Section*, 2nd ed. (Scitech Publishing, 2004).
[7]B. Chambers and A. Tennant, "Active Dallenbach radar absorber," in *APS International Symposium (Digest) (IEEE Antennas and Propagation Society)*, IEEE (2006), pp. 381–384.
[8]L. Ke, Z. Xin, H. Xinyu, and Z. Peng, "Analysis and design of multilayer Jaumann absorbers," in *IEEE International Conference on Microwave Technology and Computational Electromagnetics (ICMTCE)* (2011), pp. 81–84.
[9]B. A. Munk, *Frequency Selective Surfaces* (John Wiley & Sons, Inc., Hoboken, NJ, USA, 2000).
[10]G. Lavigne, K. Achouri, V. S. Asadchy, S. A. Tretyakov, and C. Caloz, "Susceptibility derivation and experimental demonstration of refracting metasurfaces without spurious diffraction," IEEE Trans. Antennas Propag. **66**(3), 1321–1330 (2018).
[11]N. Shitrit, I. Yulevich, E. Maguid, D. Ozeri, D. Veksler, V. Kleiner, and E. Hasman, "Spin-optical metamaterial route to spin-controlled photonics," Science **340**(6133), 724–726 (2013).
[12]N. Yu and F. Capasso, "Flat optics with designer metasurfaces," Nat. Mater. **13**(2), 139–150 (2014).
[13]A. V. Kildishev, A. Boltasseva, and V. M. Shalaev, "Planar photonics with metasurfaces," Science **339**(6125), 1232009 (2013).
[14]A. I. Kuznetsov, A. E. Miroshnichenko, M. L. Brongersma, Y. S. Kivshar, and B. Luk'yanchuk, "Optically resonant dielectric nanostructures," Science **354**(6314), aag2472 (2016).
[15]S. B. Glybovski, S. A. Tretyakov, P. A. Belov, Y. S. Kivshar, and C. R. Simovski, "Metasurfaces: From microwaves to visible," Phys. Rep. **634**, 1–72 (2016).
[16]C. L. Holloway, M. A. Mohamed, E. F. Kuester, and A. Dienstfrey, "Reflection and transmission properties of a metafilm: With an application to a controllable surface composed of resonant particles," IEEE Trans. Electromagn. Compat. **47**(4), 853–865 (2005).
[17]K. Achouri, B. A. Khan, S. Gupta, G. Lavigne, M. A. Salem, and C. Caloz, "Synthesis of electromagnetic metasurfaces: Principles and illustrations," EPJ Appl. Metamater. **2**, 12 (2015).
[18]A. A. Elsakka, V. S. Asadchy, I. A. Faniayeu, S. N. Tcvetkova, and S. A. Tretyakov, "Multifunctional cascaded metamaterials: Integrated transmitarrays," IEEE Trans. Antennas Propag. **64**(10), 4266–4276 (2016).
[19]H. Markovich, D. Filonov, I. Shishkin, and P. Ginzburg, "Bifocal Fresnel lens based on the polarization-sensitive metasurface," IEEE Trans. Antennas Propag. **66**(5), 2650–2654 (2018).
[20]Y. Ra'di, V. S. Asadchy, and S. A. Tretyakov, "Total absorption of electromagnetic waves in ultimately thin layers," IEEE Trans. Antennas Propag. **61**(9), 4606–4614 (2013).
[21]Y. Ra'di, C. R. Simovski, and S. A. Tretyakov, "Thin perfect absorbers for electromagnetic waves: Theory, design, and realizations," Phys. Rev. Appl. **3**(3), 37001 (2015).
[22]Z. Zhou, K. Chen, J. Zhao, P. Chen, T. Jiang, B. Zhu, Y. Feng, and Y. Li, "Metasurface Salisbury screen: Achieving ultra-wideband microwave absorption," Opt. Express **25**(24), 30241–30252 (2017).
[23]A. M. Mahmoud, A. R. Davoyan, and N. Engheta, "All-passive nonreciprocal metastructure," Nat. Commun. **6**, 8359 (2015).
[24]C. Pfeiffer and A. Grbic, "Metamaterial Huygens' surfaces: Tailoring wave fronts with reflectionless sheets," Phys. Rev. Lett. **110**(19), 197401 (2013).
[25]A. Epstein and G. V. Eleftheriades, "Huygens' metasurfaces via the equivalence principle: Design and applications," J. Opt. Soc. Am. B **33**(2), A31 (2016).
[26]V. Kozlov, D. Filonov, A. S. Shalin, B. Z. Steinberg, and P. Ginzburg, "Asymmetric backscattering from the hybrid magneto-electric meta particle," Appl. Phys. Lett. **109**(20), 203503 (2016).
[27]D. Filonov, B. Z. Steinberg, and P. Ginzburg, "Asymmetric micro-Doppler frequency comb generation via magnetoelectric coupling," Phys. Rev. B **95**(23), 235139 (2017).
[28]I. Shishkin, D. Baranov, A. Slobozhanyuk, D. Filonov, S. Lukashenko, A. Samusev, and P. Belov, "Microwave platform as a valuable tool for characterization of nanophotonic devices," Sci. Rep. **6**(1), 35516 (2016).
[29]D. Filonov, Y. Kramer, V. Kozlov, B. A. Malomed, and P. Ginzburg, "Resonant meta-atoms with nonlinearities on demand," Appl. Phys. Lett. **109**(11), 111904 (2016).
[30]D. S. Filonov, A. S. Shalin, I. Iorsh, P. A. Belov, and P. Ginzburg, "Controlling electromagnetic scattering with wire metamaterial resonators," J. Opt. Soc. Am. A **33**(10), 1910 (2016).
[31]P. V. Kapitanova, P. Ginzburg, F. J. Rodríguez-Fortuño, D. S. Filonov, P. M. Voroshilov, P. A. Belov, A. N. Poddubny, Y. S. Kivshar, G. A. Wurtz, and A. V. Zayats, "Photonic spin Hall effect in hyperbolic metamaterials for polarization-controlled routing of subwavelength modes," Nat. Commun. **5**, 3226 (2014).
[32]A. V. Krasavin, P. Segovia, R. Dubrovka, N. Olivier, G. A. Wurtz, P. Ginzburg, and A. V. Zayats, "Generalization of the optical theorem: Experimental proof for radially polarized beams," Light: Sci. Appl. **7**(1), 36 (2018).